

EXPERIMENTAL VALIDATION OF PHOTOVOLTAIC WATER PUMPING MODELS

Dagmar Jaehnig, S.A. Klein, and W.A. Beckman

Solar Energy Laboratory
University of Wisconsin - Madison

ABSTRACT

An experiment has been designed to measure the performance of small direct-coupled photovoltaic water pumping systems. Minute by minute measurements of water flow rate, solar radiation, ambient and cell temperatures as well as voltage and current have been recorded for several days of outdoor operation. A DC circulating pump and two photovoltaic (PV) panels from different manufacturers were tested at different static heads. A model of the PV water pumping system was developed by combining separate models for the PV array and the pump/motor unit. The PV array current-voltage characteristics are described with a 4-parameter model presented by Duffie and Beckman (1991). The combined performance of the pump and motor is described with two equations relating current, voltage, head, and flow rate as recommended by Kou (1996). Manufacturers' data were used to determine the parameters for both the PV array and pump/motor models. The models use these parameters along with measured head, radiation and temperature data to predict the pumped water flow rate. Significant differences were found between predictions and measurements. This paper investigates reasons for these discrepancies. The major discrepancies appear to be due to inaccurate data from the pump manufacturer. The variation of solar radiation absorptance of the PV panel with solar incidence angle was also found to be a factor contributing to the discrepancies.

INTRODUCTION

Small PV pumping systems can be used to pump fluid through a solar collector in a solar domestic hot water system. There are several potential advantages to a PV pumping system in this application. First, the PV array eliminates the parasitic electrical power that is used to operate a conventional pump. Second, the PV array serves not only as an energy source but also as a controller for the pump. The characteristics of the PV array and pump/motor unit allow the fluid flow rate to vary with radiation level in a non-linear manner with a threshold radiation level below which no flow occurs. These characteristics may increase the performance of a solar water heating system if the PV array and pump/motor unit are properly selected. However, because the solar radiation and ambient temperature vary

over a wide range during the annual operation of a solar water heating system, an optimum PV pumping system can only be identified by simulation methods. Models of the PV array and pump/motor unit are needed for simulations.

Mathematical models of system component performance are formulated in terms of parameters that depend on physical characteristics of the component and known operational information. The PV array and pump/motor models can be expressed in a format that uses only manufacturers' catalog information. With these models it is necessary to calculate the current voltage characteristics of PV array and the pumped flow rate as a function of weather conditions, pump head and characteristics of the hydraulic system. In this paper, the results of these calculations are compared to experimental measurements.

PV MODEL

The current voltage characteristic of a PV array is a non linear relationship. A 4 parameter model for PV arrays that is described by Duffie and Beckman (1991), uses the equivalent circuit shown in Figure 1 to represent this relationship. Using this electrical circuit, the current-voltage relationship at a specified solar radiation and cell temperature is given by

$$I = I_L - I_0 \{ \exp[(V + IR_s) / a] - 1 \} \quad (1)$$

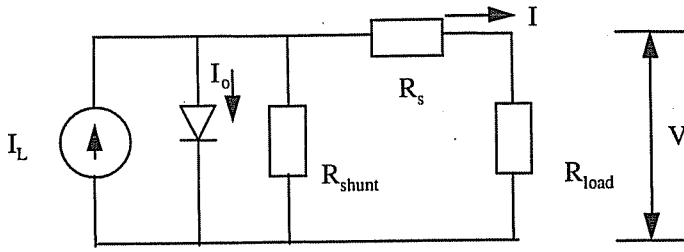


Figure 1: Equivalent circuit of a solar cell

Equation (1) assumes that the shunt resistance R_{shunt} is infinite since it is known to be a large value for crystalline cells. The light current I_L , reverse saturation current I_0 , series resistance R_s , and the fitting parameter a depend on radiation and cell temperature as indicated in equations (2) through (5). I is the current, V the voltage and I_D the diode current.

$$I_L = \left(\frac{G}{G_{ref}} \right) \cdot \left[I_{ref} + \mu_{isc} (T_c - T_{cref}) \right] \quad (2)$$

$$\frac{I_0}{I_{0ref}} = \left(\frac{T_c}{T_{cref}} \right)^3 \exp \left[\frac{N_s E_q}{a_{ref}} \left(1 - \frac{T_{cref}}{T_c} \right) \right] \quad (3)$$

$$\frac{a}{a_{ref}} = \frac{T_c}{T_{cref}} \quad (4)$$

$$R_s = R_{sref} \quad (5)$$

In the above equations, G is the solar radiation in W/m^2 , E_q is the bandgap of module material which is 1.12 eV for silicon cells, N_s is the number of cells in series in one module, T_c is the cell temperature (K) and μ_{isc} is the temperature coefficient of short-circuit current. The remaining four variables a_{ref} , I_{Lref} , I_{0ref} , and R_{sref} are parameters that must be evaluated at the reference solar radiation G_{ref} and cell temperature T_{cref} in order to apply the model.

These 4 parameters can be calculated if four current voltage pairs are known. PV manufacturers ordinarily provide performance information at only three operating conditions corresponding to open circuit, short circuit, and maximum power at reference conditions which are usually $1000 W/m^2$ solar radiation and $25^\circ C$ cell temperature. The fourth parameter can be calculated if the temperature coefficients of open circuit current μ_{voc} and short circuit voltage μ_{isc} are known. As shown in Duffie and Beckman (1991), the parameter a_{ref} can then be found in terms of these temperature coefficients using equation (6).

$$a_{ref} = \frac{\mu_{voc} T_{cref} - V_{oc} + E_q N_s}{\frac{\mu_{isc} T_{cref}}{I_{Lref}} - 3} \quad (6)$$

The model parameters a_{ref} , I_{Lref} , I_{0ref} , and R_{sref} are determined at reference conditions using manufacturer's data. Then equations (1) through (6) are used to relate current and voltage for the actual weather conditions.

PUMP/MOTOR MODEL

Kou (1996) presents a model for a pump/motor unit which relates the current, voltage, flow rate (\dot{V}) and pump head (H) with two polynomial equations represented in equations (7) and (8). The parameters in these equations must be determined by fitting manufacturer's data. Voltage is assumed to be a function of current and possibly of head as well. The flow rate can then be calculated using the second function relating flow rate, pump head and voltage.

$$v = f_1(I, H) \quad (7)$$

$$\dot{V} = f_2(V, H) \quad (8)$$

The current-voltage characteristics of the PV panel depend upon solar radiation and cell temperature. The current-voltage characteristics of the pump/motor are a function of pump head. The operating point of the direct-coupled system is found by determining the current and voltage which satisfy both the current voltage characteristics of the PV array (equation (1)) and the motor (equation (7)). The current-voltage characteristics of the PV panel depend upon solar radiation and cell temperature. The current-voltage characteristics of the PV array must be solved simultaneously with the current-voltage characteristics of the pump/motor which are a function of pump head. With the voltage thus determined, equation (8) is used to calculate the pumped flow rate as a function of head, H . Consequently, measured values of solar radiation, cell temperature and pump head are necessary to calculate the flow rate of PV pump system.

Figure 2 shows the current-voltage characteristics of a PV array at different radiation levels superimposed with the current-voltage characteristic of a pump/motor. The pump/motor characteristic starts at a particular current and voltage called the threshold of the pump. If the output of the PV array is less than this threshold value (which depends on the pump head), no fluid pumping occurs.

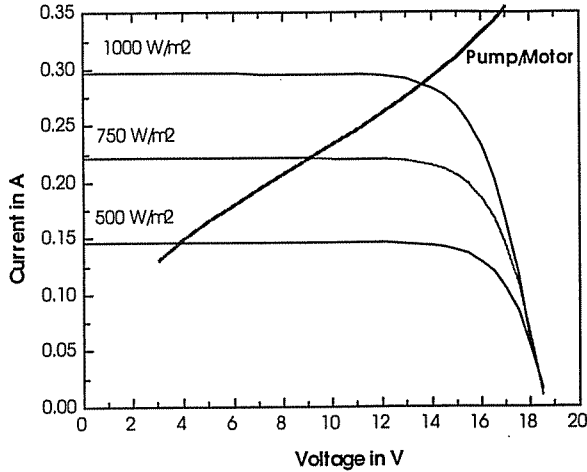


Figure 2: Current-voltage characteristics for a PV array at three radiation levels and for the pump/motor unit

For the pump used for the experiments (Laing), the catalog data indicated that the voltage was independent of head as shown in Figure 2. A 3rd order equation of the form $V=f(I)$ was found to relate current and voltage. A 3rd order equation with crossterms of the form $V = f(V, H)$ was found to adequately represent the manufacturer's data. The fitted equations are given by equations (9) and (10). Table 1 provides the coefficients used in these equations.

$$V = a_0 + a_1 \cdot I + a_2 I^2 + a_3 \cdot I^3 \quad (9)$$

$$V = b_0 + b_1 V + b_2 V^2 + b_3 V^3 + b_4 H + b_5 H^2 + b_6 H^3 + b_7 V H + b_8 V H^2 + b_9 V^2 H + b_{10} V^2 H^2 \quad (10)$$

Table 1: Parameters for the Fitted Pump Relations Equations (9 & 10)

Parameter	Value	Parameter	Value
a_0	-19.672	b_0	-1.7005
a_1	185.6548	b_1	0.6533345
a_2	-284.23	b_2	-0.039378
a_3	148.8095	b_3	0.00125198
		b_4	-4.1894
		b_5	-1.7646
		b_6	-0.026979
		b_7	0.5791779
		b_8	0.1702965
		b_9	-0.021406
		b_{10}	-0.0036076
No. of points	4	No. of points	60
Std. Dev.	0.0000216 V	Std. Dev.	0.00414 gpm

EXPERIMENTS

An experimental setup was designed to pump water from a container through a flow meter back into the container with a constant static head as depicted in Figure 3. The purpose of this experiment was to obtain actual operational data to compare with the predictions from the PV array and pump/motor models.

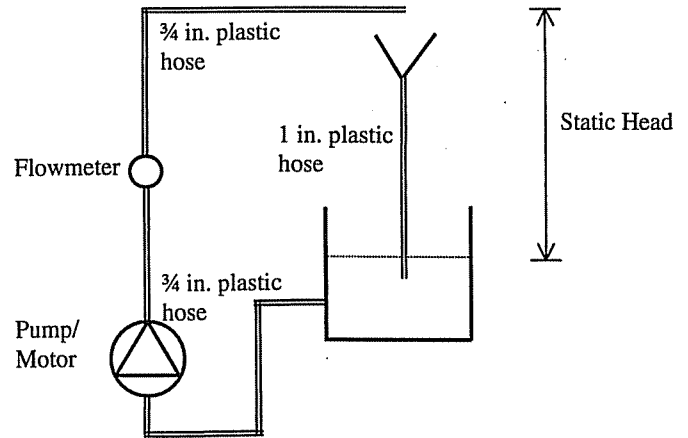


Figure 3: Hydraulic Setup for the Experiments

The pump was plumbed in series with a straight pipe, a flowmeter and then a flexible hose so to allow easy adjustments of the static head. The diameter of the hose was 19 mm. The head loss due to friction in the hose was on the order of a few millimeters and it was judged to be negligible.

The flowmeter is a Hall effect turbine flowmeter. The manufacturer states the accuracy of the flowmeter to be $\pm 1.5\%$ of the reading for flow rates between 4.2 to 75.8 l/min and $\pm 2\%$ of reading below 4.2 l/min (Omega, 1996). The head loss through the flowmeter was determined from the manufacturer's information as a function of the flow rate and this correction was applied to all measurements. The correction was on the order of a few centimeters depending on the flow rate.

The photovoltaic panel was mounted horizontally in order to reduce the uncertainty in estimating the solar radiation incident on the PV array. The radiation measurements were made next to the experimental setup. The pyranometer used is a Spectrosun Model SR-75 that has a mean uncertainty of 3.6%. Minute data of global radiation for Madison measured by the U.S. Department of Commerce National Oceanic and Atmospheric Administration (NOAA) on a horizontal surface were downloaded from NOAA to calibrate the pyranometer. Comparison of NOAA data and our own measurements using clear day data at solar elevation angles greater than 45° showed a standard deviation of only 0.12%.

Ambient and cell temperatures of the PV panels were measured. To measure the temperature of the PV array, a thermocouple was glued with a conductive aluminum-containing glue onto the back of the panel. The thermocouple was then insulated from the backside. A thermocouple was placed in the shade underneath the PV panel to measure the air temperature near the panel. The data logging system was especially designed for thermocouple inputs. It has a built in cold

junction and software that directly calculates the measured temperature given the type of thermocouple. The thermocouples used were copper-constantan that have an output of up to 20 mV. This equipment provided a resolution with the 12-bit converter of 9.78 μV which corresponds to 0.18°C. However, the uncertainty of the temperature measurement is only $\pm 1^\circ\text{C}$ due to the inherent uncertainty in the thermocouple.

To measure the current, a precision resistor of very low resistance ($0.1\Omega \pm 1\%$) was connected in series between the PV panel and the pump. The voltage across this resistor was measured with the analog input board of the data logging system. The uncertainty of the resistor causes an uncertainty of about 1% in the current measurement. The voltage across the PV panel was also measured. Because the data logging system could not measure an input greater than 10 V, the voltage was divided by two precision resistors of 1.1 M Ω and 2.15 M Ω respectively. Voltage was measured across the 1.1 M Ω resistor. Both resistors have an accuracy of $\pm 1\%$, resulting in an uncertainty in voltage of $\pm 0.9\%$. High resistances were used to minimize the current passing through the voltage measurement branch. At the maximum voltage of around 21V, the measured current was approximately 6.4 μA which was negligible compared to the operating current of the system.

A magnetically-coupled DC circulating pump (Laing) and two different PV panels (SOLAREX MSX-5L (Solarex, 1988 and Schalla, 1997) and SIEMENS SM-6) were tested. Characteristics of these system components are provided in Table 2. Measurements of current, voltage, cell temperature and head as well as solar radiation were taken at every second and averaged over one minute intervals for a range of operating conditions using a KEITHLEY 500A measurement and control system. The frequency of the square wave output signal of the flowmeter was counted by the data logging system over 20 seconds and averaged over one minute intervals. Experiments at two different heads and using two different PV panels were conducted.

Table 2: Rated Current, Voltage and Power for the PV arrays and Pump

	SIEMENS	SOLAREX	LAING
Rated current	0.39 A	0.27 A	0.26 A
Rated voltage	15 V	16.8 V	12 V
Rated power	6 W	4.5 W	3.1 W

RESULTS

All measurements show that the PV pumping system starts pumping water at a considerably lower radiation level than predicted and performs less efficiently than predicted at high radiation levels. The relative error in flow rate is between 20 and 40% for high radiation levels and becomes infinite for low radiation levels when predictions are zero, but the system actually pumps water. Figure 4 shows the results for the SIEMENS module at a pump head of 55.8 cm.

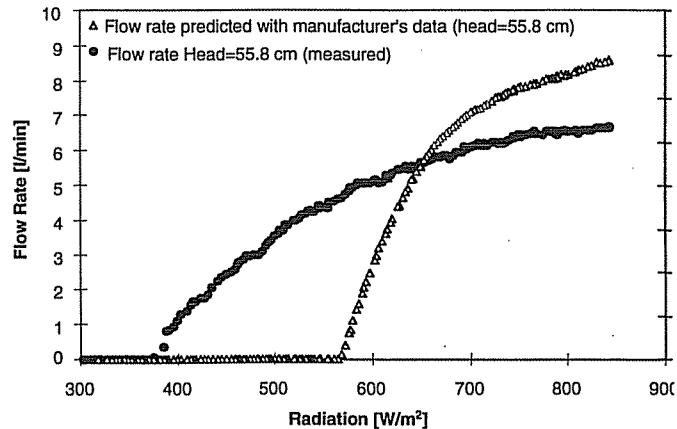


Figure 4: Measured and Predicted Flow Rate (SIEMENS SM-6)

The power output of the system determined by the PV and pump current-voltage characteristics was compared with the measured power found as the product of the measured current and measured voltage. Figure 5 shows that the model agrees very well with the experimental data for high radiation levels (difference in power less than 5%) but the model significantly underpredicts power for low radiation levels. The power output of the PV array was experimentally found to be independent of the pump head imposed on the system as suggested from the manufacturer's data. With the SOLAREX module, a small difference in power output for different heads was observed, but this difference could possibly be explained by the different ambient temperatures on the test days.

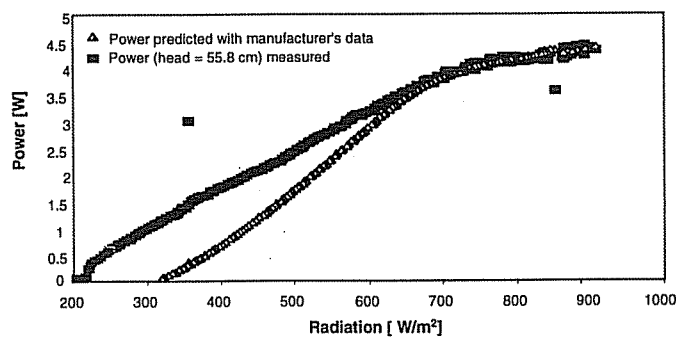


Figure 5: Measurements and Predictions of the Power Output (SIEMENS SM-6)

The PV and pump/motor models were investigated separately to determine whether the discrepancy between the experimental data and the model arises from the PV array or the pump/motor unit. For this purpose, measurements of the current-voltage curve of both PV array modules were taken using a variable resistor that allowed current-voltage data to be measured over a wide range. Simultaneous measurements of current, voltage, cell temperature and solar radiation were taken at three different radiation levels, approximately 340, 540 and 1035 W/m^2 . (There were some small variations in the solar radiation values during the measurement periods which were accounted for in the data fitting process.) The measured data were used to determine the values of the 4 parameters in the PV array model

using the method of least squares. These 'best-fit' parameters differed from the values calculated with manufacturer's data but nevertheless, the fitted model represented the data quite well with root mean square values of 0.00873 (SOLAREX) and 0.02084 (SIEMENS). However, calculated water pump rates using the PV models with the 'best-fit' parameters showed even larger discrepancies with the experimental data than found using the parameters obtained from the manufacturer's PV array and pump/motor data, except for high radiation levels around 900 W/m².

The current-voltage characteristics of the pump/motor unit were measured over a large range of operating conditions. Figure 6 shows that for high currents (high radiation levels) the measured voltages compare reasonably well to the voltage obtained from curve-fits of the manufacturer's pump/motor information, but significant discrepancies occur at low currents.

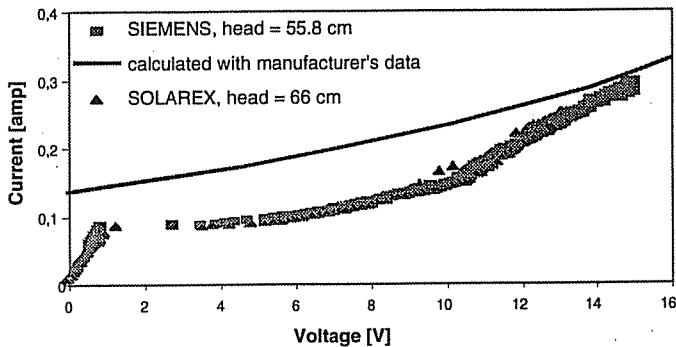


Figure 6: Operating Points: Experimental Results and Manufacturer's Data

Although the pump/motor unit may draw power (starting at voltages above 1 V), the water flow rate is zero for voltages lower than about 10 volts for the pump heads used in these experiments. A curve fit of the measured current and voltage for voltages above 10 V (where fluid begins to flow), results in a 2nd order polynomial function of the form $V=f(I)$. Using this curve-fit in place of the current-voltage relationship deduced from pump/motor manufacturer's data, significantly reduces the discrepancy between the measured and calculated power, as shown in Figure 7 for the SOLAREX array. Figure 7 shows the predictions using the least squares curve fit as well as the corrected pump current-voltage characteristics. The only significant discrepancies left are at radiation levels below 400 W/m².

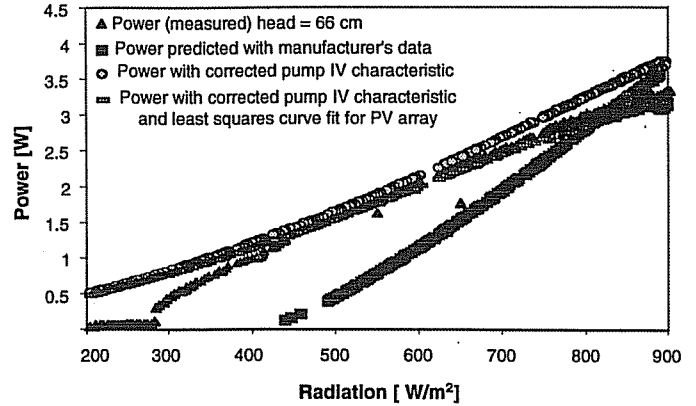


Figure 7: Corrected IV Characteristic of the Pump/Motor Unit (SOLAREX)

The influence of the incidence angle on radiation incident on the PV panels was investigated to determine if the remaining discrepancies between calculated and measured power at low radiation levels could be explained. The short circuit current of a solar cell should, in theory, be directly proportional to the radiation level. A plot of the measured short circuit currents of the two panels over the measured radiation showed that this was not the case for the experimental data. An explanation for this behavior could be that the reflection of solar radiation off the array cover at high incidence angles (early morning and late afternoon) is greater than at lower incidence angles (around noon). The low radiation values were measured at high incidence angles. The following incidence angle modifier relation was used to account for incidence angle effects.

$$K_{\tau\alpha} = \frac{(\tau\alpha)}{(\tau\alpha)_n} = 1 + b_0 \left(\frac{1}{\cos \theta} - 1 \right) \quad (11)$$

where τ - transmittance of the cover
 α - absorptance of the cells
 θ - incidence angle
 b_0 - incidence angle modifier constant.

The subscript n in equation (9) indicates normal incidence. Equation (9) is strictly valid only for incidence angles smaller than 60°. The angular dependence of the transmittance depends very much on the nature of the cover. The dependence is not known for the covers used in the tested panels. As a first-order approximation, the dimensionless transmittance-absorptance product as a function of angle of incidence was assumed to be the same as that for a nonabsorbent single glass cover having an index of refraction of 1.526 (Duffie and Beckman (1991)). (Some plastics have indices of refraction higher and some are lower than glass.) The incidence angle modifier constant b_0 was estimated using the incidence angles at the time of the solar radiation measurements. Correcting the incident radiation with the calculated incidence angle modifier and using parameters obtained with a new least squares curve fit significantly improved the calculated results for the SIEMENS module, especially for low radiation levels. Even at very high incidence angles when

equation (11) is not valid, an improvement was observed. For the SOLAREX module the predictions are not improved, but they were already within 5% of the measurements. The SOLAREX panel is covered only with a very thin bonded plastic film while the SIEMENS panel on the other hand has a hard plastic cover. The difference in cover material may explain why the two PV arrays have very different responses to changes in the solar radiation incidence angle.

Figure 8 shows the obtained power output compared with measured data and prediction made with manufacturer's data for the SIEMENS panel at a 55.8 cm pump head. The results are slightly better with the incidence angle modifier than when using manufacturer's data for the pump, especially for low radiation levels.

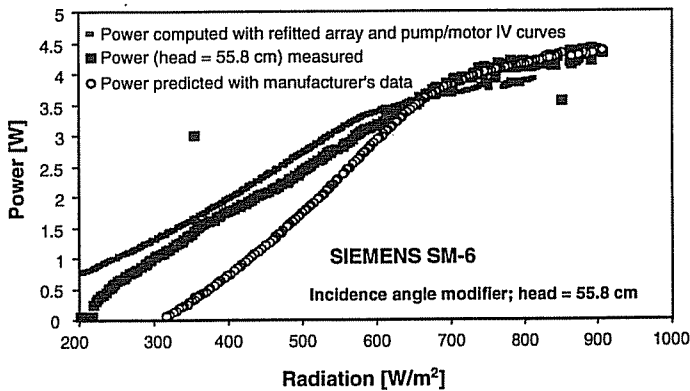


Figure 8: Prediction with Incidence Angle Modifier (SIEMENS SM-6)

One purpose of the PV array and pump/motor models is to provide estimates of the water-pumping rate as a function of operating conditions. The corrections that have been applied thus far only focus on the current and voltage of the PV array or the pump/motor unit. The water-pumping rate is a function of voltage and head. Figure 9 compares the measured flow rates with calculated flow rates determined in two ways. The curve labeled 'manufacturer's data' shows results using the original curve-fits to manufacturer's data. This curve is the same as that shown in Figure 4. The curve labeled 'Calculated flow rate' uses the best curve-fits for the current-voltage characteristics of the PV array and the pump/motor, which were based on measurements taken from this experiment.

The results in Figure 9 are disappointing. Even after using experimental data to best fit the current-voltage characteristics of the PV array and the pump/motor unit, the predicted flow rates differ significantly from the measured values, particularly at high radiation values. The problem here is due to a discrepancy between the measured flow rates and the values deduced from manufacturer's data at a given voltage and head, as seen in Figure 10. It would of course be possible to fit the flow rate as a function of voltage and head. A general curve-fit was not attempted since experimental data were taken at only two heads.

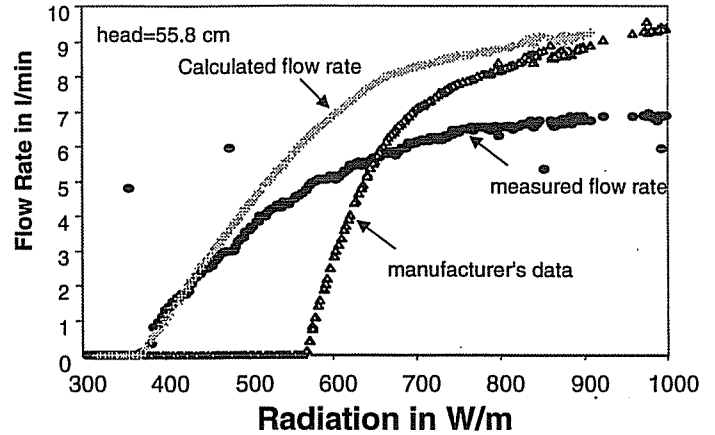


Figure 9: Predicted Flow Rate with Corrected Pump IV Characteristics

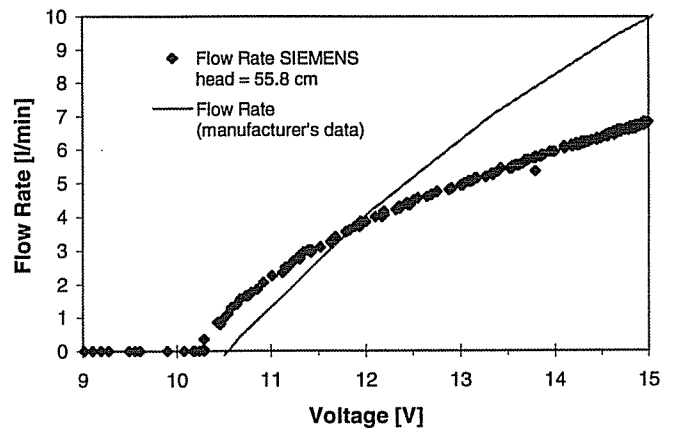


Figure 10: Flow Rate Equation of the Pump (Measured and Predicted Data)

CONCLUSIONS

An experimental setup has been designed to accurately measure the performance of a small-scale direct-coupled PV pumping system. Voltage, current, ambient and cell temperatures and radiation pump head and flow rate were all measured at one minute intervals. Tests have been performed using a DC circulating pump direct-coupled to a PV module. Two different modules were tested. Predictions of the performance of the system were made using a 4-parameter PV array model and two equations to represent the operational data for the pump/motor unit. Comparing the predictions and the measurements showed significant differences between measurements and predictions.

An investigation was conducted to determine the major cause of the discrepancies between calculated and measured flow rates. The IV characteristics of the PV modules were found to be well represented by information provided by the PV array manufacturers. However, an improvement in the predicted power of one array was observed when the effects of incidence angle were taken into consideration. The pump/motor unit was found to be the major source of discrepancies

between measured and calculated power and flow rate. The measured flow rate and power were found to not agree well with the data provided by the manufacturer for this particular pump/motor unit. Since only one unit was tested, we cannot comment on the statistical variation of the pump/motor performance.

The performance of a PV pump is dependent upon the ambient conditions in a highly non-linear manner. We have found that it was not possible to accurately estimate the flow rate of this PV driven pump system with the information provided by the manufacturer. Simulation models which can calculate the pumped flow rate as a function of operating conditions currently provide the only available means of designing optimal systems which employ solar-powered pumping equipment. Improved models for the motor/pump unit are needed for this purpose.

Schalla, Erich, SOLAREX Corporation, 1997, personal communication.\

SIEMENS Solar Industries, "Installation Guide for SIEMENS Solar M5/M10/M20 Solar Electric Modules", Camarillo, CA.

SOLAREX Corporation, 1988, "Data Sheet for MSX-30, 18, 10 and 5 Lite", Frederick, MD.

NOMENCLATURE

a	- fitting parameter
a_0 to a_3	- curve fitting parameters
b_0 to b_{10}	- curve fitting parameters
b_0	- incidence angle modifier constant
E_q	- band gap of silicon
G	- solar radiation
H	- pump head
I	- current
I_L	- light current
I_D	- diode current
I_0	- reverse saturation current
K_{α}	- incidence angle modifier
N_s	- number of cells in series in one module
R_s	- series resistance
R_{sh}	- shunt resistance
T_c	- cell temperature
V	- voltage
\dot{V}	- flow rate

Greek letters

α	- absorptance of the cells
μ	- temperature coefficient
τ	- transmittance of the cover
θ	- incidence angle

indices

sc	- short circuit
oc	- open circuit
ref	- at reference conditions

REFERENCES

- Duffie, J.A., Beckman, W.A., 1991 "Solar Engineering of Thermal Processes", 2nd edition, John Wiley & Sons, Inc. New York.
- Kou, Qing, 1996, "A Method for Estimating the Long-Term Performance of Photovoltaic Pumping Systems", M.S. Thesis, Mechanical Engineering, University of Wisconsin - Madison.
- LAING Thermotech, Inc., "Data Sheet and Installation Instructions for Laing MC-201 DC-N", Chula Vista, CA.
- OMEGA Engineering Inc., 1996, "Operator's Manual, FTB 4607", Stamford, CT.